Biochemical and Biophysical Research Communications 448 (2014) 108–113

Contents lists available at ScienceDirect

Biochemical and Biophysical Research Communications

journal homepage: www.elsevier.com/locate/ybbrc

First evidence of pathogenicity of V234I mutation of hVAPB found in Amyotrophic Lateral Sclerosis

Dhrubajyoti Chattopadhyay, Soma Sengupta *

Department of Biochemistry, University of Calcutta, India

ARTICLE INFO

Article history:
Received 10 April 2014
Available online 30 April 2014

Keywords:
ALS
Pathogenicity
Cross-linking
Ubiquitination
Cell viability

ABSTRACT

Amyotrophic Lateral Sclerosis is a motor neurodegenerative disease which is characterized by progressive loss of motor neurons followed by paralysis and eventually death. In human, VAMP-associated protein B (VAPB) is the causative gene of the familial form of ALS8. Previous studies have shown that P56S and T46I point mutations of hVAPB are present in this form of ALS. Recently, another mutation, V234I of hVAPB was found in one familial case of ALS. This is the first study where we have shown that V234I-VAPB does not form aggregate like other two mutants of VAPB and localizes differently than the wild type VAPB. It induces Ubiquitin aggregation followed by cell death. We propose that V234I-VAPB exhibits the characteristics of ALS in spite of not having the typical aggregation property of different mutations in various neurodegenerative diseases.

© 2014 Elsevier Inc. All rights reserved.

1. Introduction

Amyotrophic Lateral Sclerosis (ALS) is a neurodegenerative disease caused by motor neuron death which leads to muscle weakness, paralysis and eventually death due to respiratory failure within 3–5 years of symptom onset. ALS is classified into sporadic (SALS) and familial (FALS) form of ALS. Approximately 10% of the cases are familial while the rest are sporadic. Till date, several mutations in seven genes are known to be associated to FALS viz. superoxide dismutase (SOD1), senataxin, alsin, dynactin, TARDBP, FUS, VAPB [1–3].

VAPB is a member of the VAP family which also includes VAPA, a protein involved in vesicle trafficking [4–6]. VAPs are known to interact with the proteins involved in the regulation of sterol, lipid biosynthesis, trafficking and ER stress [7–11]. To date, three VAPB mutations (P56S, T46I and V234I) have been reported. The P56S mutation was identified in seven Brazilian kindred exhibiting clinically diverse phenotypes, including ALS and late onset spinal muscular atrophy [12]. The second mutation, T46I was found in one case of FALS in United Kingdom [13]. Recently, the third mutation, V234I was identified in one FALS patient of Dutch origin who also harbored a repeat expansion in *C9orf72* (chromosome 9 open reading frame 72), another ALS causative gene [14]. VAPB has 3 conserved domains: an N-terminal MSP (major sperm protein) domain, (amino acids 1–125), a central coiled coil domain (amino acids 158–211) and a c-terminal transmembrane domain (amino acids 220–243) [15]. The P56S and T46I mutations are both located in the MSP domain while V234I is located in the transmembrane (TMD) domain of the protein. A recent study reported that the mutant allele of V234I in *Drosophila*, DVAP-V260I exhibits the major hallmarks of the human disease including aggregate formation, reduced viability, neuromuscular defects, abnormal locomotion behavior etc. [16]. Although, the characterization and pathogenic effect of V234I-hVAPB has not been reported till date.

This is the first report where we show that V234I does not aggregate like the mutants involved in neurodegenerative diseases. The extent of aggregation and cross-linking of V234I-VAPB resembles that of WT-VAPB, not the mutant proteins. However, V234I mutation causes different localization of the protein like two other mutants of VAPB. In addition, we have demonstrated the pathogenic effects of V234I-VAPB, promoting the formation of ubiquitinated aggregates and reducing cell viability.

2. Materials and methods

2.1. Antibodies and DNA constructs

Monoclonal anti-VAPB, monoclonal anti-ubiquitin and rabbit anti-PDI antibodies were purchased from Sigma. Monoclonal

Abbreviations: ALS, Amyotrophic Lateral Sclerosis; VAMP, vesicle associated membrane protein; PDI, protein disulfide isomerase; TMD, transmembrane domain; UPR, unfolded protein response.

* Corresponding author. Present address: Department of Biochemistry, University of Calcutta, 35, Ballygunge Circular Road, Kolkata 700019, West Bengal, India.
E-mail address: ssshriya448@gmail.com (S. Sengupta).

http://dx.doi.org/10.1016/j.bbrc.2014.04.102
0006-291X/© 2014 Elsevier Inc. All rights reserved.

anti-myc antibody was from Invitrogen and Rabbit monoclonal anti-GFP antibody was purchased from Abcam. Goat anti-mouse IgG-HRP, Alexa Fluor 546-conjugated goat anti-Rabbit IgG and Alexa Fluor 546-conjugated anti-mouse IgG were from Jackson ImmunoResearch. Vectashield mounting media with DAPI was purchased from VectorLab. The vector pOTB7 containing human VAPB was purchased from Thermo Scientific. VAPB obtained from this vector by PCR was cloned into mammalian expression vectors pEGFP-N1 and pCMV-myc. Point mutations were obtained by the QuikChange XL site-directed mutagenesis kit (Stratagene) according to the manufacturer's protocol. The following VAPB mutations were established: GFP- and myc-tagged P56S, T46I and V234I. All the plasmid sequences were confirmed by sequencing.

2.2. Cell culture and solubility assay

HEK293 cells were cultured in DMEM media containing 10% FBS and 2% penicillin–streptomycin. For the solubility assay, cells were transiently transfected with the plasmids containing myc-tagged WT-VAPB, P56S-VAPB, T46I-VAPB and V234I-VAPB separately by using Profection mammalian transfection reagent (Promega) according to the manufacturer's protocol. Cells were harvested after 48 h of transfection, lysed by the lysis buffer (10 mM Tris–Cl, pH 7.4, 1% Triton X-100, 100 mM NaCl) containing 1× protease inhibitor cocktail (Sigma) and 1 mM Phenylmethylsulfonylfluoride (PMSF; Sigma) and incubated for 30 min at 4 °C. Supernatant and pellet fractions were separated by centrifugation at 13,000 rpm for 15 min. Pellets were dissolved in equal amount of lysis buffer. Samples were mixed with 4× sample buffer containing β-mercaptoethanol and boiled. Equal amounts of proteins were loaded onto 15% SDS–PAGE and subjected to western blotting on nitrocellulose membrane. After blocking, membrane was immunoblotted with anti-myc antibody (1:5000) followed by a goat anti-mouse IgG-HRP at 1:5000. Signals were detected using SuperSignal West Pico Chemiluminescent substrate (Thermo Scientific).

2.3. Chemical cross-linking

HEK293 cells were transfected with the plasmids containing myc-tagged WT, P56S, T46I and V234I-VAPBs and grown in 60 mm tissue culture plate. After 48 h of transfection, cells were incubated with 1% formaldehyde (stock solution, 37%) for 10 min at room temperature. Then the formaldehyde was quenched by 125 mM glycine for 5 min. The cells were washed three times with phosphate buffered saline (PBS) and lysed in buffer (50 mM Tris–HCl, pH 7.4, 100 mM NaCl, 2 mM EDTA, 1% Triton X-100, 1% sodium deoxycholate) containing 1× protease inhibitor cocktail and 1 mM PMSF. The cells were incubated for 30 min at 4 °C and centrifuged at 12,000 rpm for 10 min. To the pellet, lysis buffer was added, solubilized and boiled for 5 min. Both supernatant and pelleted samples were mixed with sample buffer and boiled for either 1 min or 30 min for reverse cross-linking. Equal amount of proteins were loaded onto 12% SDS–PAGE and subjected to western blotting. Membrane was immunoblotted with anti-myc antibody (1:5000) followed by a goat anti-mouse IgG-HRP at 1:5000.

2.4. Immunofluorescence experiments

HeLa cells used for these experiments were cultured with DMEM containing 10% FBS and 2% penicillin–streptomycin. Cells were transfected with the plasmids containing GFP-tagged WT-, P56S-, T46I- and V234I-VAPB, separately. Approximately 48 h or 72 h post-transfection, cells were fixed with 4% paraformaldehyde in PBS for 15 min at room temperature, blocked in PBS with 0.5% BSA and 0.02% glycine for 45 min at room temperature. Then the cells were incubated with either anti-PDI (1:125) or anti-ubiquitin (1:160) antibody for 2 h at room temperature. Following brief washing, cells were incubated with either Alexa Fluor 546-conjugated goat anti-rabbit IgG (1:200) or Alexa Fluor 546-conjugated goat anti-mouse IgG (1:400) containing 5% normal goat serum for 45 min at room temperature. The samples were mounted on glass slides with Vectashield mounting media and observed using an Olympus IX81 confocal microscope.

2.5. Cell viability assay

Neuroblastoma (N2A) cells (20,000 cells/well) were grown in a 96-well plate and the cells were transfected with the plasmids encoding myc, myc-tagged VAPB and mutants separately by using Effectene transfection reagent (Qiagen). Cells without transfection were used as control. 48-h after transfection, cells were treated with 3-(4,5-dimethyl thiazol-2-yl)-2,5-diphenyl tetrazolium bromide (MTT; sigma) at a final concentration of 100 μg/well and incubated for 4 h at 37 °C. Then the cells were solubilized in 200 μl of DMSO and incubated for 1 h in dark at room temperature with shaking followed by measuring the color of the released product formazan on a plate reader (Molecular Devices) at 570 nm where the background wavelength used was 620 nm.

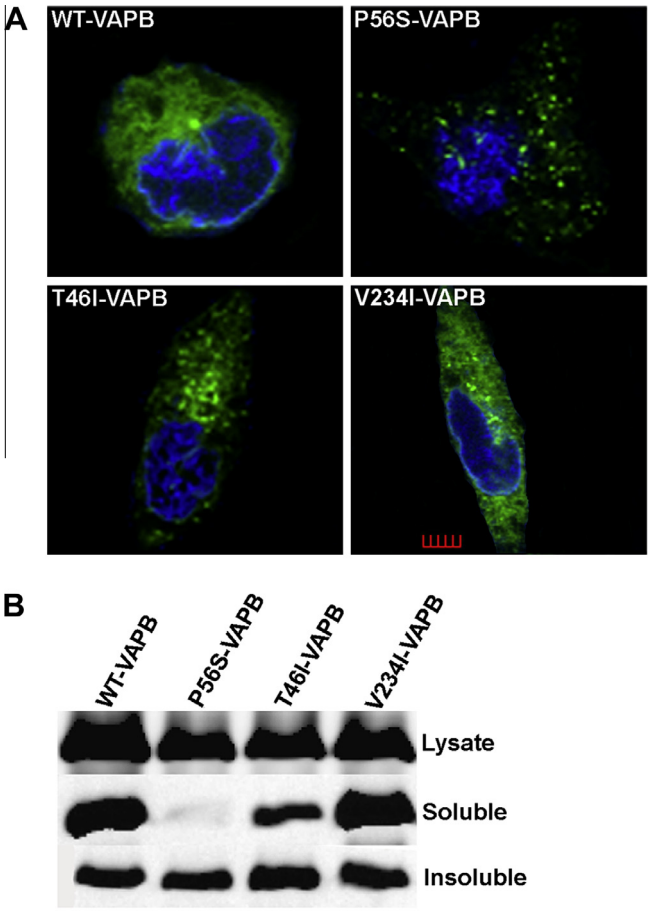

Fig. 1. V234I mutation does not induce large aggregation. (A) HeLa cells were transfected with the indicated plasmids and fixed 48 h after transfection. The distributions of the proteins are shown by GFP (green) and nuclei are shown by DAPI (blue) staining. Scale bar: 5 μm. (B) Lysates of HEK293 cells transfected with myc-tagged VAPB and its mutants, solubilized with Triton X-100, are separated into soluble and insoluble fractions. The lysates, soluble and insoluble, each fraction contains the same amount of protein. Proteins are blotted with anti-myc antibody. (For interpretation of the references to color in this figure legend, the reader is referred to the web version of this article.)

3. Results and discussion

3.1. V234I does not have aggregation property like P56S and T46I mutants of VAPB

The V234I mutation of hVAPB has recently been identified in one ALS patient of Dutch origin [14]. This newly identified mutation is located within the highly conserved and functionally important transmembrane domain whereas the previously identified P56S and T46I mutations are located in the conserved MSP domain of VAPB. The reported theoretical pathogenicity estimate of V234I mutation was 0.79 (values above 0.5 indicate pathogenicity) with a sensitivity of 0.85 and specificity of 0.93 [14]. In comparison, the pathogenicity estimate of P56S and T46I mutations were 0.62 and 0.77, respectively [13].

Abnormal aggregations of mutant proteins are pathological hallmarks of several neurodegenerative diseases such as Parkinson disease, Alzheimer disease, Huntington disease and ALS. In such diseases, large protein aggregates are formed within the cell or in extracellular plaques [17]. But, the mechanism by which the aggregates are formed is largely unknown. We tested the aggregation property of V234I-VAPB and compared with P56S-, and T46I-VAPB. As previously reported, in HeLa cells we also could not detect WT-VAPB aggregation (Fig. 1A) barring small granules/aggregates in few cells (data not shown). Surprisingly, it was observed that V234I-VAPB, like the WT protein, did not form typical aggregates but formed small granules in more number of cells compared to the WT-VAPB. The same expression pattern of V234I-VAPB was also observed in neuronal cell line, N2A (data not shown). However, a recent study reported the visible aggregation property of both WT- and V260I-VAPB in drosophila where V260I is the orthologue of V234I-hVAPB. So, our result does not agree with the reported result in drosophila. This could be attributed due to poor homology (less than 50% homology) between hVAPB and dVAPB protein sequence. As reported previously, we have also found that P56S and T46I mutants formed aggregates [13,18] but the extent of aggregation of T46I differed from that of P56S. P56S normally formed medium to large aggregates whereas T46I aggregation ranged from small granules/aggregates to medium or large aggregates although lot of cells showed no small aggregates.

Then we tested the solubility of WT and mutant VAPB proteins in non-ionic detergent, Triton X-100, to understand the biochemical properties of the proteins. In Fig. 1B, it was shown that V234I-VAPB was present both in soluble and insoluble fractions to similar extent as that of the WT protein. Like the earlier report, we identified a negligible amount of P56S in the soluble fraction which was hardly detected but we were unable to get the similar extent of P56S and T46I proteins in the soluble fraction as reported in Chen et al. [13]. Therefore, V234I although having high pathogenicity estimate of 0.79 did not show the aggregation behavior like the two aforementioned VAPB mutants.

3.2. V234I does not co-localize with PDI

VAPB was reported to predominately localize to the ER with a web-like staining pattern and co-localized with PDI, an ER resident

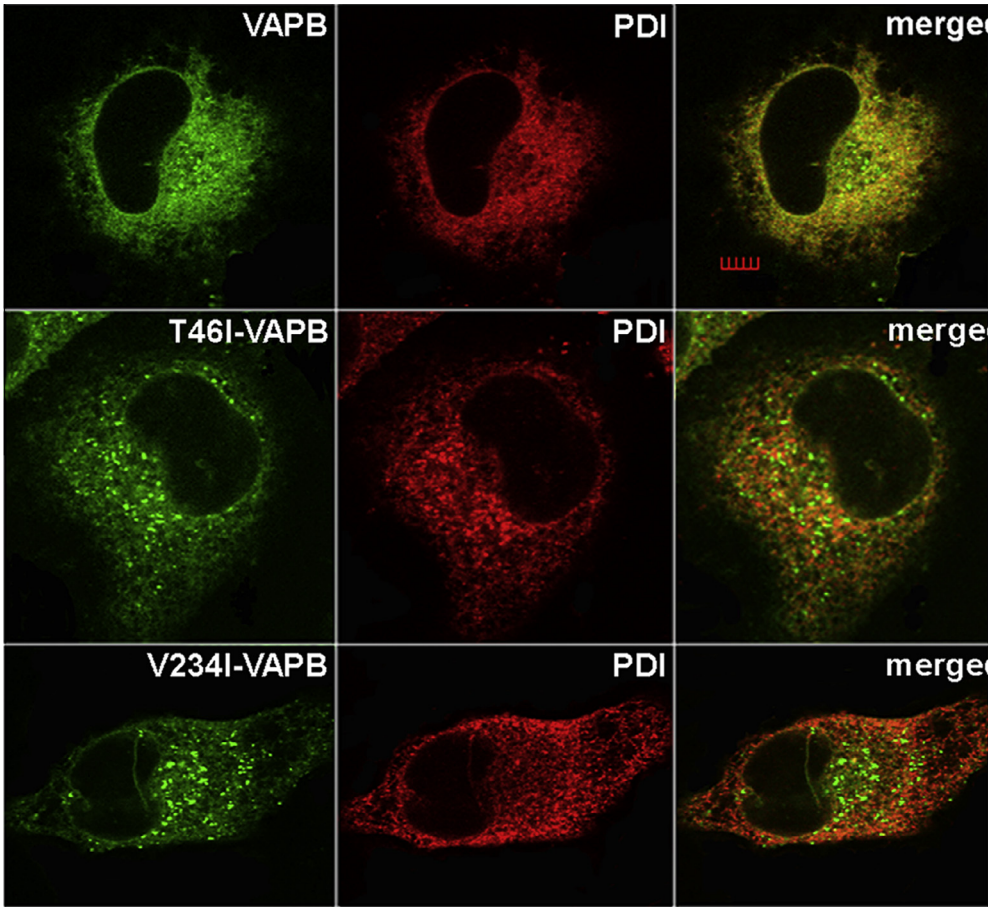

Fig. 2. V234I-VAPB does not co-localize with PDI. HeLa cells were transfected with the plasmids containing GFP-tagged WT-VAPB, T46I-VAPB or V234I-VAPB. After 48 h of transfection, cells were immunostained with anti-PDI antibody followed by Alexa-Fluor 546 conjugated goat anti-rabbit IgG. Scale bar: 5 μm. WT, T46I and V234I-VAPBs (green) and PDI (red) are merged and shown in the right side of the panel. (For interpretation of the references to color in this figure legend, the reader is referred to the web version of this article.)

protein [19]. It was also reported that P56S-VAPB aggregates did not co-localize with PDI or calreticulin, another ER marker. As the TMD of VAPB is responsible for anchoring the protein to the ER membrane we wanted to investigate whether the V234I mutation localized in the TMD affects the binding of VAPB to the ER membrane. For this purpose, we used HeLa cells to transfect with WT-, T46I-, V234I-VAPBs and after fixing we stained for endogenous PDI. As already known, we also found that WT-VAPB co-localized with PDI and predominately resided in the ER (Fig. 2). T46I mutant of hVAPB is well characterized but on the other hand, the localization of T46I-VAPB was unknown till date. We found that both T46I and V234I did not co-localize with PDI. The possible reason behind the different localization of V234I-VAPB might be due to the detachment of the protein from the ER membrane and redistribution of the protein to ER sub-compartments or other regions within the cell.

3.3. V234I mutation does not affect cross-linking of the full-length protein

The coiled-coil domain of VAPB is critical for the oligomerization [20] but the TMD also contributes to VAPB oligomerization through the dimerization motif ^{235}GXXXG^{239} where two glycine residues are separated by three amino acids on a helical framework. As the V234I mutation is located just before the dimerization motif it prompted us to investigate the effect of this mutation on VAPB oligomerization. Fig. 3A shows the oligomerization pattern of soluble fraction of WT-VAPB and its mutants. As usual WT-VAPB formed dimer and the cross-linking was reversed. As expected we could not see any monomer and dimer band for P56S-VAPB in the soluble fraction. We could see some monomer and dimer of T46I-VAPB which was reversed upon reversing the cross-links. V234I mutant formed dimer equivalent to that formed by WT protein and could also be reversed. But, no higher oligomers were detected in this fraction of the proteins. When the pelleted fractions of the cross-linked proteins were resolved we obtained same monomer and dimer patterns of WT-VAPB and its mutants on cross-linking and reverse cross-linking (Fig. 3B). WT-VAPB and V234I-VAPB formed higher oligomer which could be either trimer or tetramer. We could see very little of P56S monomer and dimer in the insoluble fraction possibly due to the formation of higher order oligomers which could be very difficult to solubilize under the condition used in this study and probably did not run in the gel.

Therefore, it could be concluded that the presence of V234I mutation in the vicinity of the dimerization motif did not affect the cross-linking of the full-length protein. To corroborate this data, we used GOR protein secondary structure prediction tool (Expasy) to evaluate the alpha helicity of VAPB and its mutants and found the number of alpha helix of V234I is increased to 75 from 71 of WT protein which probably resulted in increase or same overall compactness of V234I-VAPB compared to the WT-VAPB structure. This property was reflected in the cross-linking of WT and V234I proteins where the latter protein formed equivalent or more dimer and higher order oligomer compared to its WT counterpart. So, V234I mutation might contribute to increased helicity of the protein. Although the P56S mutant contain same number of alpha helices as the WT protein, it induced conformational changes within MSP domain and caused exposure of the hydrophobic core to the solvent [20] which enhances the propensity of the protein to oligomerize which is validated by cross-linking. T46I

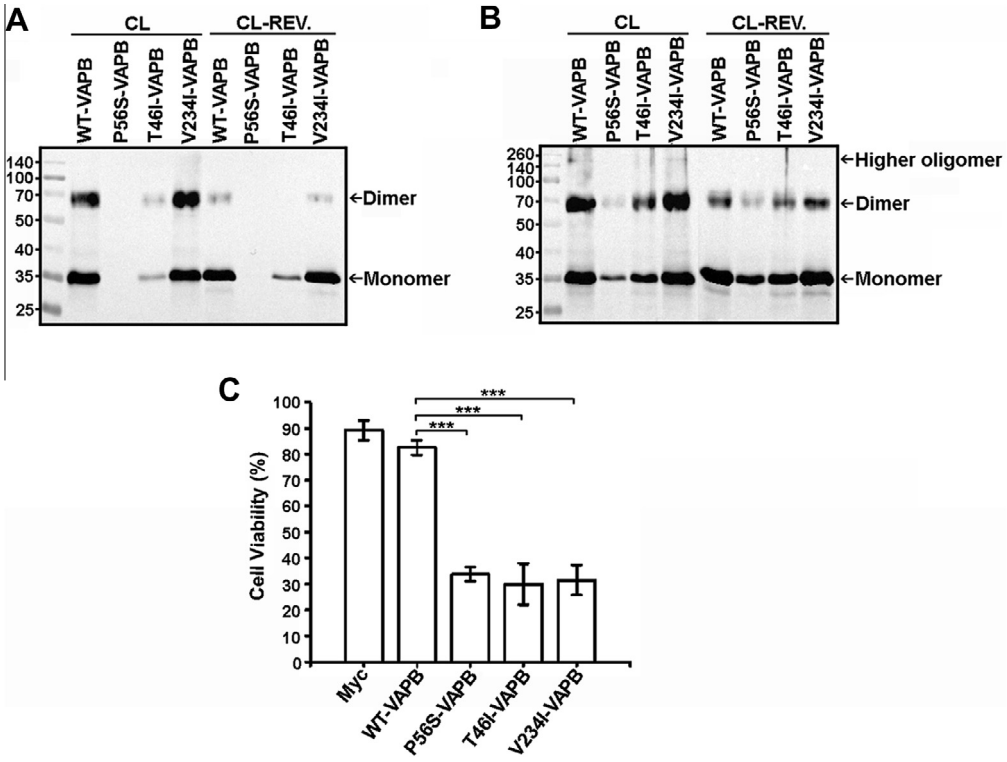

Fig. 3. V234I mutation does not affect the cross-linking of full-length protein and induces cell death. Oligomerization was done by cross-linking using formaldehyde after 48 h of transfection with myc-tagged WT-, P56S-, T46I-, V234I-VAPB plasmids into HEK293 cells. Cell lysates were separated into (A) soluble and (B) insoluble fractions. Proteins were blotted with anti-myc antibody. Monomer, dimer and higher oligomers are marked by open arrowheads. The cross-linked and reverse cross-linked proteins are denoted as CL and CL-REV, respectively. Pre-stained molecular marker, in kDa, is positioned in the left. (C) Cell viability assay was done by using MTT in N2A cell line where the cells were transfected with myc vector, myc-tagged WT and mutant plasmids. Percentage viability of myc, WT-VAPB and its mutant plasmid transfected cells was calculated by using the viability of non-transfected cells as 100%. The error bars are based on three independent experiments. The p values from one way ANOVA tests are 0.00003 (VAPB and P56S), 0.0004 (VAPB and T46I) and 0.0001 (VAPB and V234I). Bonferroni's comparison tests were applied as a post-test, and the significance is shown in the graph. Asterisks show statistical significance, $^{***}p < 0.001$.

mutant also contains same number of alpha helices and retains the native MSP structure with overall dynamics largely unaltered [21] which was also reflected in the cross-linking pattern.

3.4. V234I-VAPB enhances ubiquitin aggregation

The progression of neurodegenerative diseases such as ALS is often marked by the presence of ubiquitin aggregation in the cell. To investigate whether the V234I mutation triggered the presence of ubiquitin aggregates, N2A cells were transfected with either the plasmids containing GFP, VAPB or its mutants and 72 h after transfection, cells were fixed and immunostained for endogeneous ubiquitin. We observed large ubiquitin aggregates which were quite abundant in V234I-VAPB expressing cells (Fig. 4A-dI) like P56S- and T46I-VAPB expressing cells (Fig. 4A b-I, c-I), reported previously. We also quantified number of cells showing Ubiquitin aggregation, expressing either GFP, VAPB or its mutant proteins (Fig. 4B) and found a significant increase in the number of V234I-expressing cells containing Ubiquitin aggregates compared to the WT-VAPB expressing cells ($p = 0.00009$). As reported earlier, we also showed that the number of Ubiquitin-aggregates positive cells expressed either P56S or T46I were quite significant compared to the WT-VAPB. Although, the number of WT-VAPB positive cells showing ubiquitin aggregates is almost similar to that of GFP expressing cells.

The aggregation of ubiquitin was also found in neighboring cells which did not express any mutant proteins (Fig. 4A b-II, c-II, d-II) but the number of V234I-transfected neighboring cells containing ubiquitin aggregates was almost similar to the VAPB-transfected neighboring cells as shown in Fig. 4C. Whereas the difference in the number of either P56S or T46I negative cells showing ubiquitin aggregation and the WT protein were quite significant ($p = 0.0009$ and 0.0002, respectively) as reported. The mechanism behind the presence of ubiquitin aggregates in the non-transfected cells is not properly known but the possible hypothesis was the non-cell autonomous effect of the WT and mutant proteins on the non-transfected neighboring cells [13]. To date, V234I mutation was only identified as the third mutation of hVAPB in ALS. This report showed for the first time that V234I is capable to induce pathogenicity in ALS possibly through ubiquitin aggregation where ubiquitin aggregation is believed to be the result of ER stress and inactivation of UPR pathway in ALS. Additionally, we observed full co-localization between V234I-VAPB and ubiquitin (Fig. S1). The polyubiquitination of P56S-VAPB was reported [18], more work needs to be done to confirm the polyubiquitination of V234I-VAPB.

3.5. V234I-VAPB induces cell death

In normal cells, approximately 30% of the newly synthesized proteins in ER are misfolded/unfolded, some of them become refolded whereas the remaining misfolded/unfolded proteins cause ER stress. Under this condition, UPR is triggered by a number of chaperons and unfolded/misfolded proteins are degraded by ubiquitin/proteasome pathway. But, ubiquitin aggregation within the cell leads to inactivation of the UPR system and causes severe ER stress followed by cell death. As we confirmed the presence of ubiquitin aggregates in large number of V234I-transfected cells, this led us to investigate the consequences of ubiquitin aggregation in cells. To address this, we performed the cell viability assay and Fig. 3C showed that V234I-VAPB caused reduction in cell viability like P56S- and T46I-VAPB compared to WT-VAPB. We could see a drastic difference in cell viability i.e., the viability of cells was reduced to almost 50% when cells were transfected by V234I mutant compared to the cells transfected by WT-VAPB (ANOVA $p = 0.0001$) which strongly supports the induction of cell death caused by V234I mutation. We got similar pattern of reduced cell viability when the cells were transfected either by P56S- or T46I-VAPB compared to VAPB transfected cells (ANOVA $p = 0.00002$

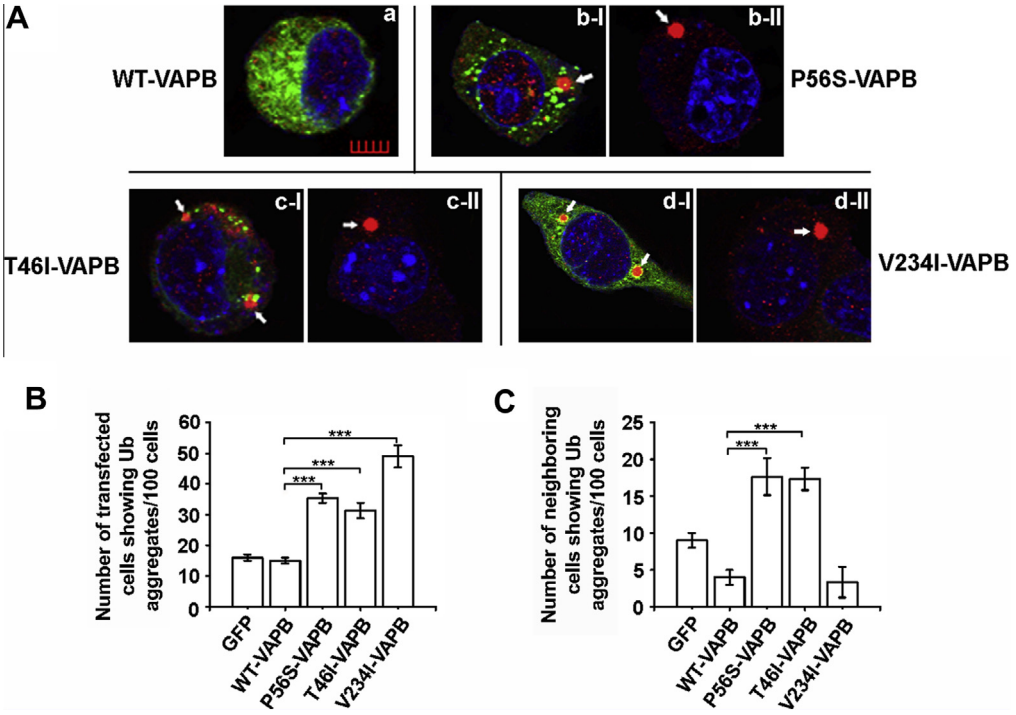

Fig. 4. V234I induces ubiquitin aggregation in mutant protein expressing cells. (A) 3 days after transfection of N2A cells with the plasmids containing GFP, GFP-tagged VAPB or its mutants, cells were fixed and stained with ubiquitin antibody for endogenous ubiquitin. Ubiquitin aggregation is shown with arrowheads in transfected cells (b-I, c-I, d-I) and in neighboring cells (b-II, c-II, d-II). Scale bar: 5 μm. The numbers of (B) transfected and (C) neighboring cells containing ubiquitin aggregates are counted on three independent experiments. The p values from one way ANOVA tests are (A) 0.00004 (VAPB and P56S), 0.0005 (VAPB and T46I), 0.00009 (VAPB and V234I) and (B) 0.0009 (VAPB and P56S), 0.0002 (VAPB and T46I). Bonferroni's comparison tests were applied as a post-test, and the significance is shown in the graph. Asterisks show statistical significance, $^{***}p < 0.001$.

and 0.0004, respectively) that is supported from published results which showed that P56S and T46I mutants induced cell death which is characteristic of ALS [13,18].

In this report, we showed for the first time the pathogenic effect of this novel mutation of hVAPB. The results demonstrated that the V234I mutation of VAPB recapitulates the phenotypes known to be associated with ALS such as ubiquitin aggregation, cell death etc. V234I is probably the only mutation which exerts pathogenic effects without forming typical aggregates in the cell in contrast to hundreds of mutations which retain the typical aggregate forming property in number of neurodegenerative diseases known so far. In comparison to P56S mutation, V234I mutant forms small aggregates/granules which might contribute to some pathogenicity in cells where the presence of small aggregates in some cells is supported by the abundance of this mutation in insoluble fraction of the protein. The V234I-VAPBs inability to co-localize with PDI pointed to the fact that this mutation is responsible for the detachment of the protein from the ER membrane. This mislocalization affects the ability of VAPB to interact with CERT, Nir proteins involved in sterol, lipid biosynthesis, trafficking which as a consequence causes dysfunction in lipid metabolism, trafficking and reduce cell viability where it is known that correct localization of VAPB is needed for the interaction with these proteins and subsequent functioning of these proteins. On the other hand, like P56S and T46I mutants, V234I-VAPB might abolish the ability of VAPB to activate the IRE1 component of the UPR pathway and thus impairing induction of ER chaperons and ERAD activity which in turn prolongs the effects of ER stress and eventually cell death occurs. Accumulation of ubiquitin aggregates reflects this ability as ubiquitin aggregation leads to impairment of ubiquitin–proteasome pathway, an active component to reduce ER stress. Additionally, the polyubiquitination of V234I-VAPB in cultured cells which might also contribute to the impairment of ubiquitin–proteasome pathway. It is evident that increased hVAPB level is sufficient to induce neurodegeneration as Gkogkas et al. [22] identified that VAPB negatively modulated the activity of ATF6, an upregulator of UPR and P56S-VAPB was a more potent inhibitor of ATF6 suggesting P56S is a loss of function mutation. T46I was also found to be a loss of function mutation. Therefore, V234I could also be considered as the loss of function mutation as it is evident from the results presented here.

Acknowledgments

This work was supported by DST (WOS-A), Government of India.

Appendix A. Supplementary data

Supplementary data associated with this article can be found, in the online version, at http://dx.doi.org/10.1016/j.bbrc.2014.04.102.

References

[1] P.A. Dion, H. Daoud, G.A. Rouleau, Genetics of motor neuron disorders: new insights into pathogenic mechanisms, Nat. Rev. Genet. 10 (2009) 769–782.
[2] C. Lagier-Tourenne, D.W. Cleveland, Rethinking ALS: the FUS about TDP-43, Cell 136 (2009) 1001–1004.
[3] P. Pasinelli, R.H. Brown, Molecular biology of amyotrophic lateral sclerosis: insights from genetics, Nat. Rev. Neurosci. 7 (2006) 710–723.
[4] D.C. Prosser, D. Tran, P.Y. Gougeon, C. Verly, J.K. Ngsee, FFAT rescues VAPA-mediated inhibition of ER-to-Golgi transport and VAPB-mediated ER aggregation, J. Cell Sci. 121 (2008) 3052–3061.
[5] L. Soussan, D. Burakov, M.P. Daniels, M. Toister-Achituv, A. Porat, Y. Yarden, Z. Elazar, ERG30, a VAP-33-related protein, functions in protein transport mediated by COPI vesicles, J. Cell Biol. 146 (1999) 301–311.
[6] J.P. Wyles, C.R. McMaster, N.D. Ridgway, Vesicle-associated membrane protein-associated protein-A (VAP-A) interacts with the oxysterol-binding protein to modify export from the endoplasmic reticulum, J. Biol. Chem. 277 (2002) 29908–29918.
[7] R. Amarilio, S. Ramachandran, H. Sabanay, S. Lev, Differential regulation of endoplasmic reticulum structure through VAP-Nir protein interaction, J. Biol. Chem. 280 (2005) 5934–5944.
[8] S.E. Kaiser, J.H. Brickner, A.R. Reilein, T.D. Fenn, P. Walter, A.T. Brunger, Structural basis of FFAT motif-mediated ER targeting, Structure 13 (2005) 1035–1045.
[9] M. Kawano, K. Kumagai, M. Nishijima, K. Hanada, Efficient trafficking of ceramide from the endoplasmic reticulum to the Golgi apparatus requires a VAMP-associated protein-interacting FFAT motif of CERT, J. Biol. Chem. 281 (2006) 30279–30288.
[10] M. Ngo, N.D. Ridgway, Oxysterol binding protein-related Protein 9 (ORP9) is a cholesterol transfer protein that regulates Golgi structure and function, Mol. Biol. Cell 20 (2009) 1388–1399.
[11] N. Rocha, C. Kuijl, R. van der Kant, L. Janssen, D. Houben, H. Janssen, W. Zwart, J. Neefjes, Cholesterol sensor ORP1L contacts the ER protein VAP to control Rab7-RILP-p150 Glued and late endosome positioning, J. Cell Biol. 185 (2009) 1209–1225.
[12] A.L. Nishimura, M. Mitne-Neto, H.C. Silva, A. Richieri-Costa, S. Middleton, D. Cascio, F. Kok, J.R. Oliveira, T. Gillingwater, J. Webb, P. Skehel, M. Zatz, A mutation in the vesicle-trafficking protein VAPB causes late-onset spinal muscular atrophy and amyotrophic lateral sclerosis, Am. J. Hum. Genet. 75 (2004) 822–831.
[13] H.J. Chen, G. Anagnostou, A. Chai, J. Withers, A. Morris, J. Adhikaree, G. Pennetta, J.S. de Belleroche, Characterization of the properties of a novel mutation in VAPB in familial amyotrophic lateral sclerosis, J. Biol. Chem. 285 (2010) 40266–40281.
[14] M. van Blitterswijk, M.A. van Es, M. Koppers, W. van Rheenen, J. Medic, H.J. Schelhaas, A.J. van der Kooi, M. de Visser, J.H. Veldink, L.H. van den Berg, VAPB and C9orf72 mutations in 1 familial amyotrophic lateral sclerosis patient, Neurobiol. Aging 33 (2950) (2012) e1–e4.
[15] S. Lev, D. Ben Halevy, D. Peretti, N. Dahan, The VAP protein family: from cellular functions to motor neuron disease, Trends Cell Biol. 18 (2008) 282–290.
[16] M. Sanhueza, L. Zechini, T. Gillespie, G. Pennetta, Gain-of-function mutations in the ALS8 causative gene VAPB have detrimental effects on neurons and muscles, Biol. Open. 15 (2014) 59–71.
[17] C.A. Ross, M.A. Poirier, Protein aggregation and neurodegenerative disease, Nat. Med. 10 (Suppl.) (2004) S10–S17.
[18] K. Kanekura, I. Nishimoto, S. Aiso, M. Matsuoka, Characterization of amyotrophic lateral sclerosis-linked P56S mutation of vesicle-associated membrane protein-associated protein B (VAPB/ALS8), J. Biol. Chem. 281 (2006) 30223–30233.
[19] E. Teuling, S. Ahmed, E. Haasdijk, J. Demmers, M.O. Steinmetz, A. Akhmanova, D. Jaarsma, C.C. Hoogenraad, Motor neuron disease-associated mutant vesicle-associated membrane protein-associated protein (VAP) B recruits wild-type VAPs into endoplasmic reticulum-derived tubular aggregates, J. Neurosci. 27 (2007) 9801–9815.
[20] S. Kim, S.S. Leal, D. Ben Halevy, C.M. Gomes, S. Lev, Structural requirements for VAP-B oligomerization and their implication in amyotrophic lateral sclerosis-associated VAP-B(P56S) neurotoxicity, J. Biol. Chem. 285 (2010) 13839–13849.
[21] S. Lua, H. Qin, L. Lim, J. Shi, G. Gupta, J. Song, Structural, stability, dynamic and binding properties of the ALS-causing T46I mutant of the hVAPB MSP domain as revealed by NMR and MD simulations, PloS One 6 (2011) e27072.
[22] C. Gkogkas, S. Middleton, A.M. Kremer, C. Wardrope, M. Hannah, T.H. Gillingwater, P. Skehel, VAPB interacts with and modulates the activity of ATF6, Hum. Mol. Genet. 17 (2008) 1517–1526.